Biophysical Journal Volume 68 April 1995 1574–1582

Fluorescence Lifetime-Based Sensing in Tissues: A Computational Study

Christina L. Hutchinson,* J. R. Lakowicz,‡ and Eva M. Sevick-Muraca*

*Purdue University, School of Chemical Engineering, West Lafayette, Indiana 47907, and ‡The Center of Fluorescence Spectroscopy, Department of Biological Chemistry, University of Maryland, Baltimore, Maryland 21201 USA

ABSTRACT We have numerically solved the photon diffusion equation to predict the distribution of light in a tissue model system with a uniform concentration of fluorophore. Our results show that time-dependent measurements of light propagation can be used to monitor the fluorescent lifetimes of a uniformly distributed fluorophore in tissues. With proper referencing, frequency-domain measurements of phase-shift, θ, may allow quantitation of fluorescent lifetimes, τ, independent of changes in the local absorption and scattering properties. These results point to a new approach for noninvasive diagnostic monitoring through quantitation of fluorescent lifetime, τ, when the lifetime of the fluorophore is comparable with photon migration times.

NOMENCLATURE

c	Speed of light in the media (cm/s)
D	Optical diffusion coefficient (cm)
f	Modulation frequency (MHz)
g	Mean cosine of the scattering angle
$I_{x,m}(\rho, t)$	Time-dependent excitation and fluorescent light intensity (#photons/(cm^2 s))
$M_{x,m}(\rho, f)$	Amplitude modulation
$N_{a_{x,m}}(\rho, t)$	Number of photons per unit volume
$P(\rho, f)$	Power spectrum from Fourier transform
t	Time (s)
t'	Fluorescent excitation time (s)
$\theta_{x,m}(\rho, f)$	Phase-shift due to the excitation or emission light propagation
θ_{total}	Phase-shift detected at the surface
θ_τ	Phase-shift due to fluorescent lifetime
$\lambda_{x,m}$	Excitation and emission wavelengths (nm)
$\mu_{am\rightarrow}$	Absorption coefficient for the emission light due to the local concentration of chromophores (cm^{-1})
$\mu_{ax\rightarrow}$	Absorption coefficient of the excitation light due to local concentration of chromophores (cm^{-1})
$\mu_{ax\rightarrow m}$	Absorption coefficient of the excitation light due to the local concentration of fluorescent probes (cm^{-1})
$\mu'_{sx,m}$	Scattering coefficient for excitation and emission light (cm^{-1})
ρ	Position
$\Phi(\rho,t)$	Fluence rate at point ρ and time t (#photons/(cm^2 s))
τ	Fluorescent lifetime (in general) (s)
τ_s	Fluorescent lifetime of the sample probe (s)
τ_{ref}	Fluorescent lifetime of the reference probe (s)
Subscripts	
x	Excitation light
m	Emission light

INTRODUCTION

Recent advances in fiber-optic, laser diode, and detector technology make possible noninvasive, biochemical sensing of tissues from the fluorescence of endogenous and exogenous probes. Although fluorescent intensity measurements may be technologically simple, these techniques suffer from distortion of emission spectra because of the wavelength-dependent scattering and absorption properties of tissues (Keijzer et al., 1989; Durkin et al., 1994). Algorithms have been developed to deconvolve the emission spectra from tissue reflectance or transmittance measurements (Wu et al., 1993; Durkin et al., 1994); however, additional measurements are required for model inputs of tissue scattering and absorption.

A second approach, lifetime-based chemical sensing, has been proposed by several investigators for the quantitation of pO_2 (Bacon and Demas, 1987; Vanderkooi et al., 1987; Wilson et al., 1983; Lippitsch et al. 1988; Carraway et al., 1991; Rumsey et al., 1991), pH (Draxler et al., 1993; Lakowicz and Szmacinski, 1993), Ca^{2+} (Lakowicz and Szmacinski, 1993), glucose (Lakowicz and Szmacinski, 1993), and other metabolites. The lifetime of a fluorescent probe may be affected by either a collision or via a energy transfer process in which energy is transferred from a fluorescent donor to an acceptor. When the process is collisional, measurements of probe lifetime, τ, can be used to determine the metabolite concentration, $[Q]$, from the Stern-Volmer relationship

$$\tau_0/\tau = 1 + \tau_0 k_q [Q], \quad (1)$$

where τ and τ_0 are the decay times with and without quencher and k_q is the quenching constant. When multi-exponential decays describe collisional quenching, different analyses must be performed (Sharma et al., 1992). When the lifetime is dependent upon the transfer of energetic states between a donor and an acceptor, local metabolite concentrations can be determined when the energy transfer is influenced by concentration. Regardless of the relaxation process, dynamic measurements of probe lifetimes for determination of metabolite concentration may prove to be a powerful diagnostic and clinical tool (Lakowicz and Szmacinski, 1993; Szmacinski and Lakowicz, 1992). The recent development of optical probes with excitation and emission spectra in the near-infrared region suggest the use of lifetime-based sensing in tissue.

Received for publication 25 May 1994 and in final form 10 January 1995.

Address reprint requests to Dr. Eva M. Sevick-Muraca, School of Chemical Engineering, Purdue University, West Lafayette, IN 47907. Tel.: 317-494-4050; Fax: 317-494-0805; E-mail: sevick@ecn.purdue.edu.

0006-3495/95/04/1574/09 $2.00

However, lifetime measurements are currently confined to dilute, nonscattering samples of probe and analyte using time- and frequency-domain analyses (for review, see Lakowicz, 1983). In the time-domain, an incident impulse of excitation light results in fluorescent emission light intensity that decays exponentially according to the lifetime of the optical probe:

$$I_m(t) = I_0 \exp(-t/\tau), \tag{2}$$

where I_0 is the emission intensity at time 0 and $I_m(t)$ is the time-dependent emitted fluorescent intensity. Equation 2 is valid when the decay of the re-emitted light intensity can be represented as a single-exponential decay time. In the frequency-domain measurement, the source of excitation light is sinusoidally modulated at a frequency f. The re-emitted light is also modulated at frequency f, but is amplitude-demodulated by a factor M, and phase-shifted by θ, with respect to the incident excitation source. The phase-shift is dependent upon the lifetime by the following expression:

$$\theta_m(f) = \tan^{-1}(2\pi f\tau) \tag{3}$$

when the activated fluorescent state can be represented in terms of a single exponential. In contrast to fluorescent intensity measurements, fluorescent lifetime measurements are independent of fluorophore concentration and excitation and emission light losses. Therefore, lifetime-based sensing may permit quantitative spectroscopic information without the artifacts due the calibration of excitation light intensity, light losses, and changes in fluorescent probe concentration (Szmacinski and Lakowicz, 1992).

However, scattering can distort measurements of τ when the lifetime of the optical probe is comparable with the "time-of-flight" associated with the migration of the excitation and fluorescent photons within the tissues or other random media (Patterson et al., 1989); then both time- and frequency-domain techniques will predict τ erroneously. Fig. 1 illustrates the time delays that comprise the time-dependent measurement of fluorescent light intensity re-emitted from tissues. Time delays are caused by: (i) the transport of excitation photons from the source to the probe embedded in the random media; (ii) the lifetime of the probe; and (iii) the transport of fluorescent photons from the fluorophore to the detector located on the tissue surface. Because probe lifetimes are on the order of 1–20 ns, accurate lifetime determinations depend upon the deconvolution of photon migration times from time-dependent measurements. When the probe lifetime is orders of magnitude greater than the photon migration times, we have shown that the origin of re-emitted signal is confined to sub-surface tissue regions (Sevick-Muraca et al., 1994; Sevick-Muraca and Burch, 1994). Thus, deconvolution of photon migration times of *short-lived* fluorophores from time-dependent measurements is necessary for lifetime-based spectroscopic interrogation *deep* within tissues or other random media.

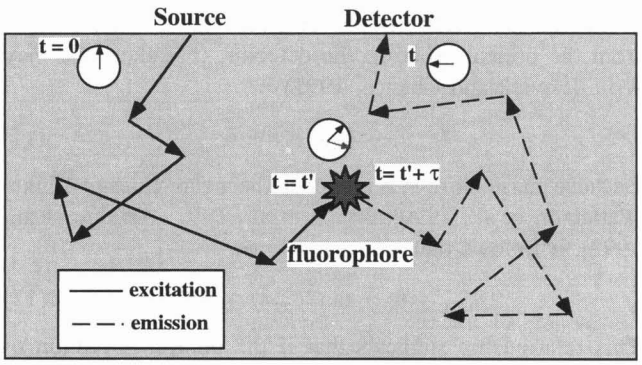

FIGURE 1 The processes for photons migration of excitation light, absorption by fluorophore, re-emission, and migration of fluorescent light to point detector. Excitation of fluorophore occurs at time t', re-emission of fluorescent photon occurs at time $t' + \tau$, and detection of fluorescent photon occurs at time t.

In this work, we show that the time-dependent measurements of fluorescent light intensity re-emitted from tissue may be used to determine probe lifetime, τ, when the lifetime is comparable with photon migration times. Our goal is to quantitate probe lifetimes independent of the time-dependent photon migration associated with excitation and fluorescent light. Because local changes in blood flow and interstitial fluid flow may alter the absorption and scattering properties of tissue, the success of this technology depends upon quantitating fluorescent lifetimes independent of any variation in photon transport caused by local changes in optical properties.

In the next section, we present the theoretical background for predicting time-dependent measurements of excitation and emission light propagation within a random media containing a uniform concentration of lifetime-sensitive probes. Afterwards, we describe an approach by which photon migration times can be deconvolved from these measurements to determine probe lifetimes. Finite element computations verify our approach and suggest a simple means for quantitative, lifetime-based sensing in tissues and other random media.

THEORY

Light propagation in tissues or other random media can be described in terms of the diffusion approximation to the radiative transport equation (Patterson et al., 1989). The diffusion equations describing the transport of excitation and emission light can be written (Patterson and Pogue, 1994; Sevick-Muraca et al., 1994; Burch et al., 1994)

$$\frac{\partial \Phi_x(\rho, t)}{\partial t} - D_x c \nabla^2 \Phi_x(\rho, t) + (\mu_{ax\to m} + \mu_{ax\to}) c \Phi_x(\rho, t) = 0 \tag{4a}$$

$$\frac{\partial \Phi_m(\rho, t)}{\partial t} - D_m c \nabla^2 \Phi_m(\rho, t) + \mu_{am\to} c \Phi_m(\rho, t) - \frac{c}{\tau} \phi \mu_{ax\to m} \int_0^t \exp\left(\frac{-(t-t')}{\tau}\right) \Phi_x(\rho, t') \partial t' = 0, \tag{4b}$$

where $\Phi_x(\rho, t)$ and $\Phi_m(\rho, t)$ are fluence rates or the flux of excitation (subscript x) and emission (subscript m) light. The

fluence rate, $\Phi_{x,m}(\rho, t)$ (photons/cm^2 s), is defined as the number of photons per unit volume at point ρ and time t ($N_{a_{x,m}}$), multiplied by the speed of light in the medium, c (cm/s), as given by Eq. 5.

$$\Phi_m(\rho, t) = N_{a_{x,m}}(\rho, t)c. \quad (5)$$

The first terms on the left-hand side of Eqs. 4a and 4b describe the accumulation rate of photons at point ρ and time t. The second term of both equations represents the diffusive or "random walk" transport of light, where D_x is the optical diffusion coefficient for excitation light (cm)

$$D_x = \frac{1}{3([\mu_{ax\rightarrow} + \mu_{ax\rightarrow m}] + (1 - g)\mu_{sx})} \quad (6a)$$

and D_m is the diffusion coefficient for emission light (cm)

$$D_m = \frac{1}{3(\mu_{am\rightarrow} + (1 - g)\mu_{sm})}, \quad (6b)$$

where μ_a represents the absorption coefficient (cm^{-1}) and $(1 - g)\mu_s$ represents the isotropic scattering coefficient (cm^{-1}). The third term in Eq. 4a accounts for the loss of excitation photons due to absorption by chromophores and the lifetime-sensitive probe, where $\mu_{ax\rightarrow}$ is the absorption coefficient associated with the local concentration of chromophores and $\mu_{ax\rightarrow m}$ is the absorption coefficient associated with the local concentration of optical probes at the excitation wavelength, λ_x. In Eq. 4b, the third term accounts for the loss of emission photons due to absorption by the local concentration of chromophores, where $\mu_{am\rightarrow}$ is the absorption coefficient due to chromophores at the emission wavelength, λ_m. The fourth term in Eq. 4b describes the time-dependent generation of emission light that results after the absorption of excitation light. The generation of emission fluence at time t that arises from excitation at t' can be described by a source term that is written in terms of the quantum efficiency of the probe, ϕ, its local concentration (as represented by $\mu_{ax\rightarrow m}$), the excitation fluence rate at the time of excitation ($\Phi_x(\rho, t')$), and an exponential term describing the decay of emission

$$S(\rho, t) = \frac{c}{\tau}\phi\mu_{ax\rightarrow m}\int_0^t \exp\frac{-(t - t')}{\tau}\Phi_x(\rho, t')\partial t'. \quad (7)$$

The total emission fluence generated at time t results from the excitation of probes with excitation times, t', ranging from times 0 to t. Therefore, the fourth term in Eq. 4b is obtained by integrating over all possible excitation times, t', ranging from 0 to t. Because of the complex integration involved in Eq. 4b, a direct analytical solution is not possible (Patterson and Pogue, 1994). However, by replacing the integral with a summation over all times, a solution for the reaction can be obtained using numerical methods.

Prediction of time-domain measurements

Upon coupling Eqs. 4a and 4b, the fluence distributions of excitation and emission light after an incident impulse can be solved. Although the exact boundary conditions cannot be incorporated into the diffusion equation, it has been long recognized that useful approximations, such as an extrapolated boundary with a negative photon source, or zero fluence ($\Phi = 0$) at the surface aptly predicts the re-emission of light from tissues. Although the zero fluence may not be the physically correct boundary condition, it nonetheless predicts the time-dependent re-emission from tissues (Madsen et al., 1992). For this reason, we use the zero fluence boundary condition in our solutions for excitation and emission light propagation in our tissue phantoms. From these fluence distributions, the time-dependent light intensities, $I_x(\rho, t)$ and $I_m(\rho, t)$ can be determined from Fick's law

$$I_{x,m}(\rho, t) = -D_{x,m}\nabla\Phi_{x,m}(\rho, t). \quad (8)$$

Prediction of frequency-domain measurements

Conversion of the time-dependent intensities into frequency-domain parameters can be accomplished by simply taking the Fourier transform of the excitation and emission intensities and computing the power spectrum, $P_{x,m}(\rho, f)$

$$P_{x,m}(\rho, f) = \int_0^\infty I_{x,m}(\rho, t)\exp(-i2\pi ft)\partial t. \quad (9)$$

The frequency-domain parameter of phase-shift, $\theta_{x,m}(\rho, f)$, can then be computed from the real and imaginary parts of the power spectrum

$$\theta_{x,m}(\rho, f) = \tan^{-1}\frac{\mathbf{Im}\,P_{x,m}(\rho, f)}{\mathbf{Re}\,P_{x,m}(\rho, f)}. \quad (10)$$

In summary, both time- and frequency-domain fluorescence measurements can be predicted from the diffusion approximation to light transport in random media.

APPROACH

Accurate lifetime-based sensing requires deconvolution of photon migration times from time-dependent measurements. If one considers the total mean time delay, $\langle t_{total}\rangle$, between the incident impulse and the detector to be comprised of the sum of time delays caused by (i) photon migration of excitation light from the source to an embedded optical probe, $\langle t_x\rangle$; (ii) probe lifetime, τ; and (iii) photon migration of emission light from the optical probe to the detector, $\langle t_m\rangle$, then one may write (Sevick and Chance, 1991)

$$\langle t_{total}\rangle = \langle t_x\rangle + \tau + \langle t_m\rangle \quad (11)$$

Because phase-shift, θ, is related to the mean "time-of-flight" (Patterson et al., 1990; Sevick et al., 1991; Arridge et al., 1992), it follows that

$$\theta_{total} = \theta_x + \tan^{-1}(2\pi f\tau) + \theta_m. \quad (12)$$

This relationship suggests that if the photon migration of excitation and fluorescent photons could be quantitated, then the fluorescent lifetimes may be obtained from frequency-domain measurements of phase-shift. Specifically, if phase-shift measurements were "referenced" to measurements in

the presence of a probe with a constant and known lifetime, τ_{ref}, then τ_s could be determined directly from a "referenced" phase-shift or phase-shift difference, $\Delta\theta$

$$\Delta\theta = \theta_s - \theta_{ref} = \tan^{-1}(2\pi f\tau_s) - \tan^{-1}(2\pi f\tau_{ref}). \quad (13)$$

Equation 13 assumes that the photon migration at the excitation and emission wavelengths for the lifetime-sensitive probes and "reference" probes are equal. A discussion of this criteria is given below.

METHOD

To verify our approach to lifetime-based sensing in tissue, a computational study was performed. The coupled set of diffusion equations (Eqs. 4a and 4b) were solved to predict the excitation and emission fluence distributions that resulted from an impulse point source on the surface of a two-dimensional (2-D) square tissue phantom, 10 cm wide × 10 cm high. Solutions for three-dimensional (3-D) models were not conducted because of the rigorous mesh generation and increased computation times associated with these types of problems. It is important to note that the 2-D model with a point source does not represent a 3-D model with a point source; rather it represents a 3-D model with a line source. Because of this, 2-D computations may not match actual experiments using a point source. Nevertheless, the scope of this work was not to make a comparison with actual measurements, but rather to determine whether lifetime-based sensing in random media is possible.

Finite element computations were performed on a Sun SPARCstation 10 using the software application FIDAP 7.0 (Fluid Dynamics International, Evanston, IL) (Suddeath et al., 1993). Computation times required up to 6 h to determine fluences for "times-of-flights" up to 100 ns. At the boundaries of the square phantom, the condition of zero fluence was assumed for the excitation and fluorescent light. As described previously, although the zero fluence boundary condition does not accurately represent a physical model, it is believed to be a reasonable approximation for this study. A single, isotropic point source of an impulse of excitation light was simulated by imposing an initial condition on a single node located one scattering length under the surface. A similar approach has been used to approximate surface illumination with light absorbing boundary conditions via the method of images using analytical expressions (Patterson et al., 1989). This assumes that photons incident to the surface are isotropically scattered after one scattering length, which is an approximation that has been shown to predict optical signals re-emitted from tissues. Excitation and emission light intensities $I_x(\rho, t)$ and $I_m(\rho, t)$ were computed from fluence rates via Eq. 8. Values of phase-shift, θ_{total}, from the emission light were determined from the FFT using Eq. 10. An evenly distributed concentration of fluorophores was assumed (e.g., the photosensitizer AISPC) to be present throughout the sample. Using the fluorescence emission spectrum for AISPC (Patterson and Pogue, 1994) and assuming a concentration of 0.1 μg/ml, the absorption coefficient due to the fluorophores, $\mu_{ax\rightarrow m}$, was calculated to equal 0.005 cm^{-1}. We have also conducted computations with partial current boundary conditions (Hutchinson et al., 1995). The final results were identical to those obtained using the zero fluence boundary condition. The quantum efficiency, ϕ, was chosen to be 0.58 for all the calculations. The fluorophore lifetime, τ, was varied from 0 to 7 ns; the absorption coefficient for the excitation and emission light, $\mu_{ax\rightarrow,am\rightarrow}$, was varied from 0.002 to 0.02 cm^{-1}; and the isotropic scattering coefficient was varied from 10 to 40 cm^{-1}. These particular coefficients were chosen because of physiological relevance. Results are shown for a single, isotropic point detector located a distance ρ away from the source in 2-D geometry.

Computations were conducted for variation in (i) the fluorophore lifetime, τ; (ii) the absorption coefficient for excitation and emission light, $\mu_{ax\rightarrow,am\rightarrow}$; and (iii) the isotropic scattering coefficient for excitation and emission light, $\mu'_{sx,m}$ to evaluate their contributions to the time-dependent photon migration characteristics of excitation and fluorescent light. Table 1 shows the parameters used to investigate the contributions of τ, $\mu_{ax\rightarrow,am\rightarrow}$, and $\mu'_{sx,m}$ on time-dependent measurements of photon migration.

To determine whether frequency-domain measurements of phase-shift can be used to quantitate fluorophore lifetime, phase-shift differences were computed and compared with Eq. 13.

RESULTS AND DISCUSSION

Effect of fluorophore lifetime, τ_s

Fig. 2 *A* illustrates the predicted measurements of the re-emitted emission light intensity, $I_m(t)$ vs. "time-of-flight." Results are presented as normalized intensities plotted as a function of fluorophore lifetime, τ_s. As expected, the increase in fluorophore lifetime resulted in the broadening of the fluorescent "time-of-flight" distribution. Results are presented for re-emitted emission intensity, 1.65 cm away from the source input on the phantom surface.

Fig. 2 *B* shows the corresponding phase-shift of the re-emitted light, θ_{total}, versus modulation frequency. Results are presented as a function of fluorophore lifetime, τ_s. Again, as expected, an increase in fluorophore lifetime results in an increase in phase-shift. The resulting phase-shift values exceed 90° because of excitation and emission photon migration.

TABLE 1 Parameters used in finite element computations

Variable	Effect of τ on $\Phi_m(\rho, t)$	Effect of $\mu_{ax\rightarrow,\ am\rightarrow}$ on $\Phi_m(\rho, t)$	Effect of $\mu'_{sx,\ m}$ on $\Phi_m(\rho, t)$
$\mu'_{sx,m}$	10	20	10.0, 20.0, 40.0
$\mu_{ax\rightarrow,\ am\rightarrow}$	0.002	0.002, 0.02	0.002
$\mu_{ax\rightarrow m}$	0.005	0.005	0.005
ϕ	0.58	0.58	0.58
τ (ns)	3.0, 5.0, 7.0	3.0, 7.0	3.0, 5.0, 7.0

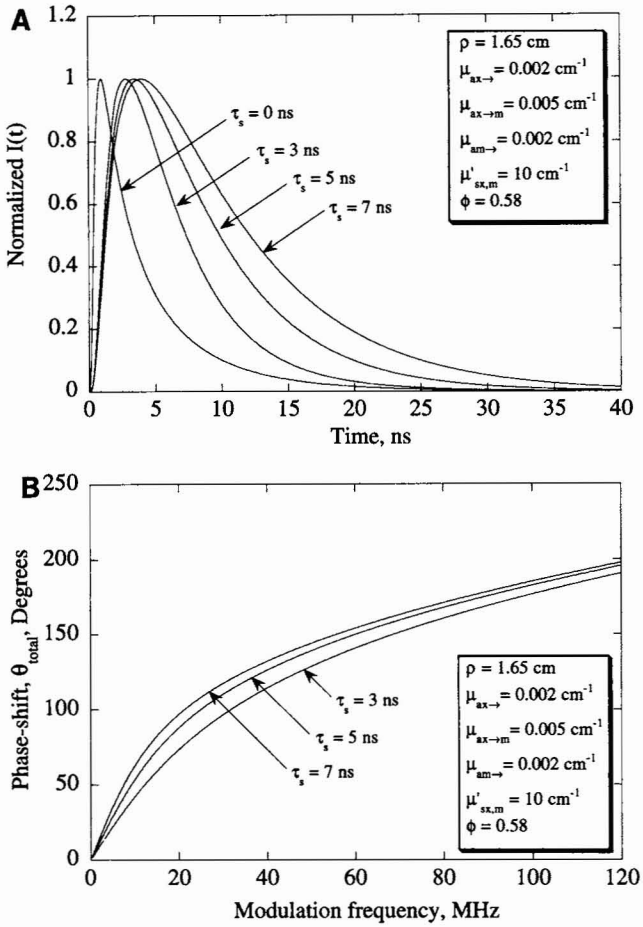

FIGURE 2 (*A*) Normalized fluorescent intensity, $I_m(\rho,t)$, which results from a uniformly distributed fluorophore with lifetime, τ_s, which varies between 1 and 7 ns. Optical properties are specified in the legend. (*B*) The phase-shift of re-emitted light, θ_{total}, versus modulation frequency which results from a uniformly distributed fluorophore with lifetime, τ_s, which varies from 1 to 7 ns. Optical properties are specified in the legend.

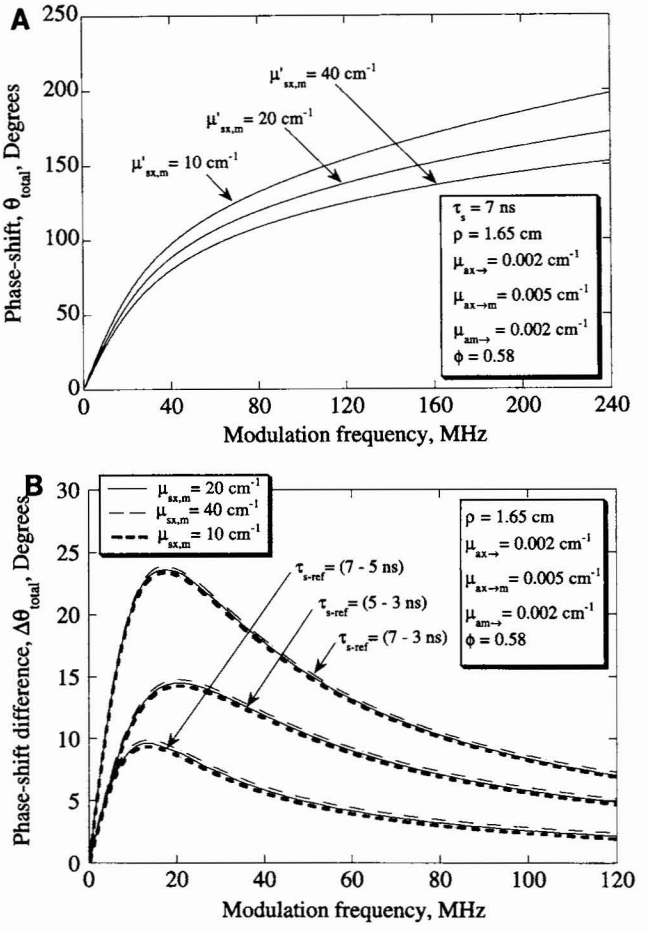

FIGURE 3 (*A*) Predicted values of phase-shift, θ_{total}, versus modulation frequency for a uniformly distributed fluorophore with lifetime equal to 7 ns. Results are presented as a function of excitation and emission scattering coefficients. (*B*) Predicted values of phase-shift difference, $\Delta\theta_{total}$, versus modulation frequency for a uniformly distributed sample and reference fluorophore. Results are presented for sample and reference fluorophore lifetimes of (i) 7 and 5 ns, (ii) 5 and 3 ns, (iii) 7 and 3 ns as a function of excitation and emission scattering coefficients.

The effect of scattering upon fluorophore lifetime determination

Previous measurements of photon migration show that an increase in tissue scattering causes an increase in the phase-shift of the re-emitted light (Patterson et al., 1990; Sevick et al., 1991; Wilson et al., 1992). This behavior is expected, because photons that are increasingly scattered will travel longer "times-of-flight" and longer optical path lengths before detection. In our computational experiments, the phase-shift of re-emitted fluorescent light is also increased when the scattering coefficient associated with emission light, μ'_{sm}, is increased whereas μ'_{sx} remained constant (data not shown). However, Fig. 3 *A* shows that when the scattering coefficient for both excitation and emission photons ($\mu'_{sx,m}$) is increased from 10 cm^{-1} to 20 and 40 cm^{-1}, the phase-shift of re-emitted fluorescent light is decreased. These results can be explained in the following manner: as the scattering coefficient for excitation light, μ'_{sx}, is increased, the gradient of excitation light at the tissue surface becomes more steep. For the case of a uniformly distributed fluorophore, the region containing the highest concentration of *excited* fluorophore will coincide with the region of highest excitation fluence. Therefore, as the scattering coefficient of excitation light, μ'_{sx}, increases, the region containing the highest concentration of *excited* fluorophore will be located closer to the tissue surface. As a result, the photon migration time will make smaller contributions to the time-dependent measurements of re-emitted light as the excitation scattering coefficient is increased. Computations showing the localization of re-emitted fluorescent signals are the subject of a companion paper (Sevick-Muraca et al., 1994; Sevick-Muraca and Burch, 1994).

Nonetheless, the goal of lifetime-based sensing is to determine τ_s independent of photon migration and independent of changes in tissue-scattering properties. Values of phase-shift at lifetimes of 3, 5, and 7 ns were obtained for scattering coefficients of 10, 20, and 40 cm^{-1}, similar to that shown in Fig. 3 *A*. As described previously, "referenced" values of phase-shift were determined by taking the difference

between phase-shift values obtained at two different lifetimes. For example, the bottom set of curves in Fig. 3 *B* ($\tau_{s-ref} = 7 - 5$ ns) shows the phase-shift difference obtained by subtracting θ_{total} when the sample fluorophore was present ($\tau_s = 7$ ns) from θ_{total} when the reference fluorophore was present ($\tau_{ref} = 5$ ns). The solid, dotted, and dashed lines in this bottom set of curves corresponds to the phase-shift differences for each of the three scattering coefficients considered ($\mu'_{sm} = 10$, 20, and 40 cm^{-1}). The match between Eq. 13 and the finite element computations is exact. Therefore, changes in photon migration due to scattering differences do not affect the phase-shift when properly referenced. For illustrative purposes, the lines were offset by adding a small increment (0.005) to the $\mu'_{sm} = 40$ cm^{-1} curve and subtracting it from the $\mu'_{sm} = 10$ cm^{-1} curve. The remaining curves in Fig. 3 *B* show that the referencing procedure works for any combination of sample and reference fluorophore lifetime.

The effect of the absorption ($\mu_{ax\rightarrow}$ and $\mu_{am\rightarrow}$) upon fluorophore lifetime determination

In addition to changes in scattering, changes in absorption can also cause altered photon migration. Fig. 4 *A* illustrates θ_{total} versus modulation frequency for two different absorption coefficients (0.002 and 0.02 cm^{-1}) for a fluorophore with a 7-ns lifetime. The fluorophore concentration remained constant, whereas the changes in absorption coefficient reflected changes in chromophore concentration. Excitation and emission absorption coefficients due to chromophores were set equal. The scattering coefficients were held constant at 20 cm^{-1}. As expected, an increase in absorption resulted in a reduction in the phase-shift because excitation and emission photons tended to travel shorter "times-of-flight" or shorter optical path lengths (Sevick et al., 1991).

The referencing procedure was also used to determine whether changes in photon migration due to absorption differences could be subtracted from lifetime-based sensing measurements. Phase-differences were computed for a sample fluorophore with a 7-ns lifetime and a reference fluorophore with a constant lifetime of 3 ns. Fig. 4 *B* shows that the phase-shift differences were independent of absorption. The solid and dotted lines correspond to the phase-shift differences computed at different absorption coefficients. These lines were artificially offset to show that changes in photon migration due to changes in absorption do not affect the phase-shift differences when properly referenced.

The effect of source-to-detector separation, ρ, upon fluorophore lifetime determination

In addition to changes in scattering and absorption, changes in source-detector separation, ρ, can cause altered photon migration. Fig. 5 *A* illustrates the phase-shift of the fluorescent light, θ_{total}, versus modulation frequency for ρ equal to 1.65 and 1.065 cm. The scattering and absorption properties were held constant. As expected, increasing the source-to-

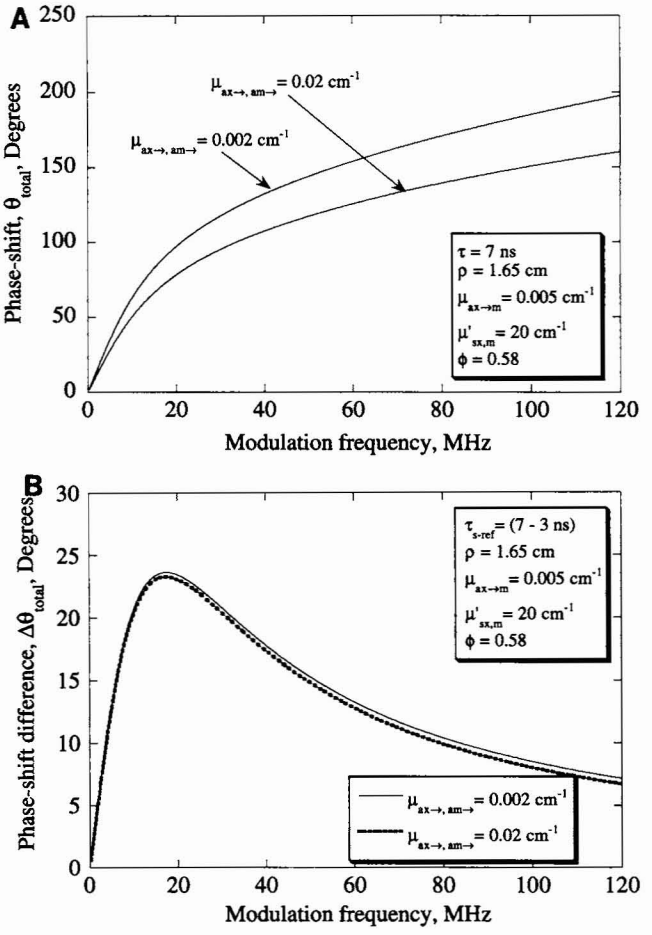

FIGURE 4 (*A*) Predicted values of phase-shift, θ_{total}, versus modulation frequency for a uniformly distributed fluorophore with lifetime equal to 7 ns. Results are presented as a function of excitation, and emission absorption coefficients due to chromophores. (*B*) Predicted values of phase-shift difference, $\Delta\theta_{total}$, versus modulation frequency for a uniformly distributed sample, and reference fluorophore. Results are presented for sample and reference fluorophore lifetimes of (i) 7 and 5 ns, (ii) 5 and 3 ns, and (iii) 7 and 3 ns as a function of excitation and emission absorption coefficients.

detector separation results in an increase in the photon "time-of-flight" which, in turn, increases the phase-shift.

To investigate whether the changes in photon migration due to changes in source-detector separation could be referenced out of lifetime-based sensing measurements, phase-differences were computed for a sample fluorophore with a 7-ns lifetime and a reference fluorophore with a constant lifetime of 3 ns. Fig. 5 *B* shows that the phase-shift differences were independent of source-detector separation. The lines were artificially offset to show that changes in photon migration due to changes in source-to-detector separation do not affect the phase-shift differences when properly referenced.

Determination of fluorophore lifetime

The results presented above suggest that the contribution of photon migration can be eliminated from lifetime-

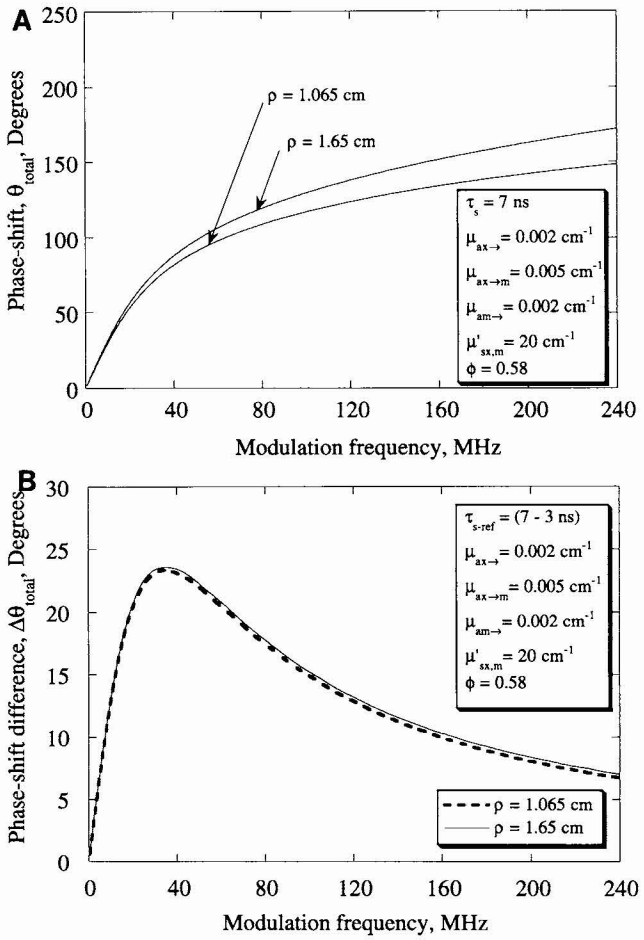

FIGURE 5 (*A*) Predicted values of phase-shift, θ_{total}, versus modulation frequency for a uniformly distributed fluorophore with lifetime equal to 7 ns. Results are presented at source-to-detector separations of 1.65 and 1.065 cm. (*B*) Predicted values of phase-shift difference, $\Delta\theta_{total}$, versus modulation frequency for a uniformly distributed sample and reference fluorophore. Results are presented for sample and reference fluorophore lifetimes of 7 and 3 ns as a function of source-to-detector separation.

based sensing measurements in tissues if proper referencing is performed. Referencing requires the presence of a second fluorophore with known and constant lifetime. Fig. 6 illustrates that the computed values of phase-shift difference can be predicted from the relationship, $\Delta\theta = \tan^{-1}(2\pi f\tau_s) - \tan^{-1}(2\pi f\tau_{ref})$.

The effect of experimental error in lifetime determination

The effect of experimental noise in the lifetime measurement was modeled by assuming an ample 0.1° error in phase-shift for both the reference and sample fluorescent signals. This would lead to a maximum 0.2° change in phase-shift when the two signals are subtracted from each other. The predicted lifetime can be calculated easily by modifying the phase-shift equation ($\theta = \tan^{-1}(2\pi f\tau)$)

$$\tau_s = \frac{\tan[\pi/180(0.2 + 180/\pi \tan^{-1}(2\pi f\tau_{s(actual)}))]}{2\pi f}. \quad (14)$$

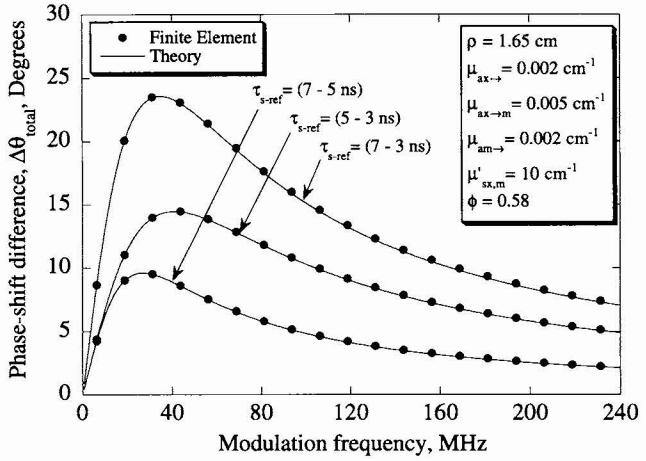

FIGURE 6 Predicted values of phase-shift, θ_{total}, and values of phase-shift predicted from $\tan^{-1}(2\pi f\tau_s) - \tan^{-1}(2\pi f\tau_{ref})$ versus modulation frequency for a uniformly distributed fluorophore with lifetime equal to 7 ns.

The percent error due to the estimated noise is shown in Fig. 7. For frequencies greater than 50 MHz, as the lifetime of the probe increases, the percent error ((measured lifetime − actual lifetime)/(actual lifetime) × 100%) increases. At higher frequencies, this effect is even more prominent. This trend can be explained by examining a plot of phase-shift for different fluorescent lifetimes (Fig. 8). As frequency increases, the phase-shift due to the probe lifetime approaches 90°. Therefore, a small change in phase-shift results in a large error in the predicted lifetime. For frequencies lower than 50 MHz, the opposite is true: the percent error is greatest at short lifetimes. At low frequencies, this error occurs because a 0.2° change results in a large variation in predicted lifetime. Our study is concerned with fluorescent lifetimes <10 ns and frequencies <250 MHz. For these conditions, the error is less than 5%.

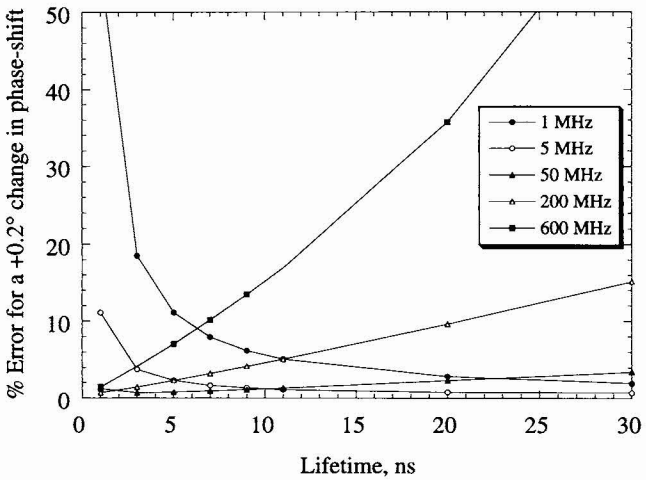

FIGURE 7 Percent error in the calculated lifetime versus actual lifetime for a +0.2° change in phase-shift. Values are calculated using the phase-shift expression $\theta_{total} = \tan^{-1}(2\pi f\tau_s)$.

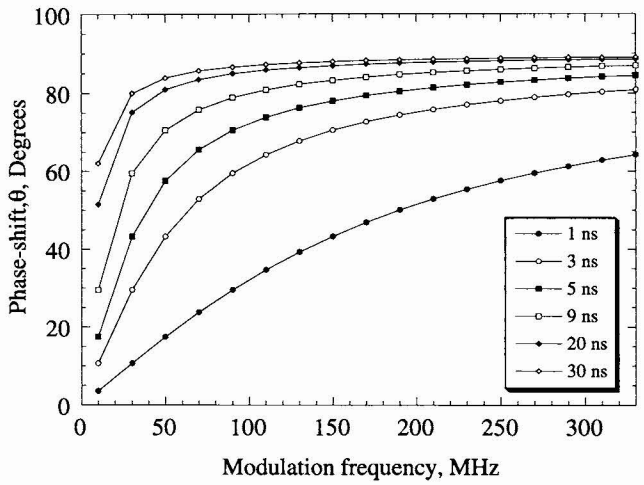

FIGURE 8 Calculated values of phase-shift versus modulation frequency for several different fluorescent lifetimes.

The error incurred due to violations of our assumption that the photon migration characteristics for the sample and reference probes had to be identical, was also analyzed. When the photon migration associated with the sample and reference probes are not the same, then the phase-shift difference, θ_{total}(sample) − θ_{total}(reference), would not equal the phase-shift associated with the lifetime of the fluorophore. Instead, there would be an unknown phase-shift due to the difference in the photon migration. Fig. 9 shows the percent error as a function of the variation in phase-shift due to violation of our assumption for several modulation frequencies when $\tau_{s(actual)}$ = 5 ns. As expected, as the variation in phase-shift increased, the percent error increased. Also, as the frequency increased, the percent error increased. Currently, we are assessing changes in absorption and scattering across various excitation and emission wavelengths to emphasize the sensitivity of our assumptions in lifetime determination. However, because scattering changes dominate photon migration in tissue and because scattering is a very weak function of wavelength in the near infrared potential for accurate lifetime-based sensing with the proposed referencing procedure is promising.

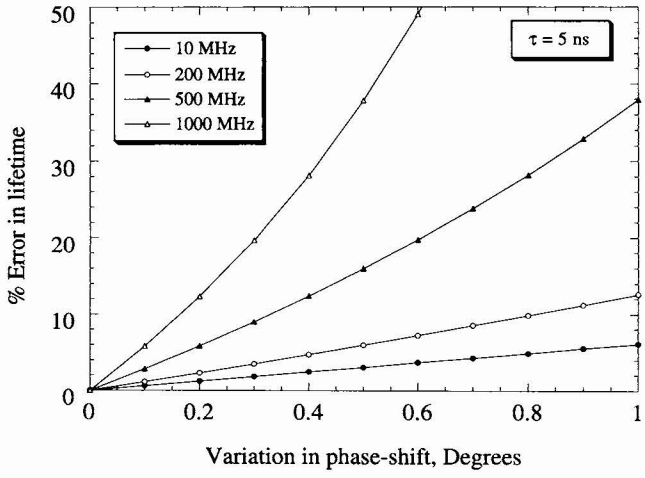

FIGURE 9 Percent error in the calculated lifetime versus variation in phase-shift for a constant lifetime of 5 ns.

CONCLUSIONS

Our results show that upon properly "referencing" frequency-domain measurements of phase-shift, θ_{total}, against measurements made with a probe of known and constant lifetime, τ_{ref}, the lifetime of a "sample" probe could be used to interrogate metabolite concentration in tissues or other random media. There have been three major assumptions made in our approach: (i) that the sample and reference probes possess similar excitation and emission spectra so that the contribution of photon migration times is identical in the measurements of sample and reference lifetime; (ii) that a fluorophore with known and constant lifetime can be identified; and (iii) that the signals arising from the sample and reference probes can be identified separately from one another. Although these criteria may seem significant, one can imagine a system in which the sample and reference probes are temporally or spatially distinct from one another. In other words, at one sampling time, the sample probe is present, and at a later time the reference probe is then administered. Likewise, the sample and reference probes may be immobilized separately from one another so that excitation light is directed to one or the other. Preliminary data suggest that our approach of lifetime-based sensing works equally well with a nonuniform distribution of optical probes (Hutchinson et al., 1995).

We have shown that the determination of lifetime from frequency-domain measurements requires either (i) "referencing" against a known and constant fluorophore, or (ii) previous knowledge of the phase-shift due to excitation and emission light. Unlike measurements of fluorescent intensity on turbid media, a priori information of tissue absorption and scattering is not needed. It is likely that this advantage will promote the biochemical sensing fluorescence lifetime-based measurements for economical, noninvasive diagnosis.

Thanks are given to Mr. Lee Suddeath and Ms. Tamara Troy for their review, and to Britton Chance, Richard Haskell, Henryk Szmacinski, and Bruce Tromberg for their input.

This work was supported in part by the Whitaker Foundation, National Institutes of Health (R01CA61413), and the National Science Foundation Young Investigator Program (E. M. Sevick-Muraca).

REFERENCES

Arridge, S. R., M. Cope, and D. T. Delpy. 1992. The theoretical basis for the determination of optical path lengths in tissue: temporal, and frequency analysis. *Phys. Med. Biol.* 37:1531–1560.

Bacon, J. R., and J. N. Demas. 1987. Determination of oxygen concentrations by luminescence quenching of a polymer-immobilized transition-metal complex. *Anal. Chem.* 59:2780–2785.

Burch, C. L., J. R. Lakowicz, and E. M. Sevick-Muraca. 1994. Biochemical sensing in tissues: determination of fluorescent lifetimes in multiply scattering media using frequency-domain fluorescence spectroscopy. *SPIE.* 2135:286–299.

Carraway, E. R., J. N. Demas, B. A. DeGraff, and J. R. Bacon. 1991. Photophysics, and photochemistry of oxygen sensors based on luminescent transition-metal complexes. *Anal. Chem.* 63:337–342.

Draxler, S. D., M. E. Lippitsch, and M. J. P. Leiner. 1993. Optical pH sensors using fluorescence decay time. *Sensors Actuators B.* 11:421–424.

Durkin, A. J., S. Jaikumar, N. Ramanujam, and R. Richards-Kortum. 1994. Relation between fluorescence spectra of dilute, and turbid samples. *Appl. Opt.* 33:414–423.

Hutchinson, C. L., T. L. Troy, and E. M. Sevick-Muraca, 1995. Fluorescence spectroscopy and imaging in random media. *SPIE.* In press.

Keijzer, M., R. R. Richards-Kortum, S. L. Jacques, and M. S. Feld. 1989. Fluorescence spectroscopy of turbid media: autofluorescence of the human aorta. *Appl. Opt.* 28:4286–4292.

Lakowicz, J. R. 1983. Principles of Fluorescence Spectroscopy. Plenum Press, New York.

Lakowicz, J. R., and H. Szmacinski. 1993. Fluorescence lifetime-based sensing of pH, Ca^{2+}, K^{+}, and glucose. *Sensors Actuators B.* 11:133–143.

Lippitsch, M. E., and S. Draxler. 1993. Luminescence decay-time-based optical sensors: principals, and problems. *Sensors Actuators B.* 11: 97–101.

Lippitsch, M. E., J. Pusterhofer, M. J. P. Leiner, and O. S. Wolfbeis. 1988. Fibre-optic oxygen sensor with the fluorescence decay time as the information carrier. *Anal. Chim. Acta.* 205:1–6.

Madsen, S. J., B. C. Wilson, M. S. Patterson, Y. D. Park, S. L. Jacques, and Y. Hefetz. 1992. Experimental tests of a simple diffusion model for the estimation of scattering, and absorption coefficients of turbid media from time-resolved diffuse reflectance measurements. *Appl. Opt.* 31:3509–3517.

Patterson, M. S., B. Chance, and B. C. Wilson. 1989. Time-resolved reflectance, and transmittance for the non-invasive measurement of tissue optical properties. *Appl. Opt.* 28:2331–2336.

Patterson, M. S., J. Moulton, B. Wilson, and B. Chance. 1990. Applications of time-resolved light scattering measurements to photodynamic therapy dosimetry. *SPIE.* 1203:62–75.

Patterson, M. S., and B. W. Pogue. 1994. A mathematical model for time-resolved, and frequency-domain fluorescence in biological tissue. *Appl. Opt.* 33:1963–1974.

Rumsey, W. L., R. Iturriaga, D. Spergel, S. Lahiri, and D. F. Wilson. 1991. Optical measurements of the dependence of chemoreception on oxygen pressure in the cat carotid body. *Am. J. Physiol.* 261:C614–C622.

Sevick, E. M., and B. Chance. 1991. Photon migration in a model of the head measured using time-, and frequency-domain techniques: potentials for spectroscopy, and imaging. *SPIE.* 1431:84–96.

Sevick, E. M., B. Chance, J. Leigh, S. Nioka, and M. Maris. 1991. Quantitation of time-, and frequency- resolved optical spectra for the determination of tissue oxygenation. *Anal. Biochem.* 195:330–351.

Sevick-Muraca, E. M., and C. L. Burch. 1994. The origin of phosphorescent signals re-emitted from tissue. *Opt. Lett.* 19:1928–1930.

Sevick-Muraca, E. M., L. F. Suddeath, and C. L. Burch. 1994. The origin of fluorescent, and phosphorescent signals re-emitted form tissues. *SPIE.* 2137:673–683.

Sharma, A., S. Draxler, and M. E. Lippitsch. 1992. Time-resolved spectroscopy of the fluorescence quenching of a doner-acceptor pair by halothane. *Appl. Phys. B.* 54:309–312.

Suddeath, L., V. Sahai, A. Wisler, C. Burch, B. Chance, and E. M. Sevick. 1993. Finite element solution of the "forward imaging" problem associated with time- and frequency-domain measurements of photon migration. *SPIE.* 1888:117–128.

Szmacinski, H., and J. R. Lakowicz. 1992. Lifetime-based sensing using phase-modulation fluorometry. *ACS Symp Ser.* 538:196–225.

Vanderkooi, J. M., G. Maniara, T. J. Green, and D. F. Wilson. 1987. An optical method for measurement of dioxygen concentration based upon quenching of phosphorescence. *J. Biol. Chem.* 262:5476–5482.

Wilson, B. C., E. M. Sevick, M. S. Patterson, and B. Chance. 1992. Time-dependent optical spectroscopy, and imaging for biomedical applications. *Proc. IEEE.* 80:918–930.

Wilson, D. F., W. L. Rumsey, T. J. Green, and J. M. Vanderkooi. 1988. The oxygen dependence of mitochondrial oxidative phosphorylation measured by a new optical method for measuring oxygen concentration. *J. Biol. Chem.* 263:2712–2718.

Wu, J., M. S. Feld, and R. P. Rava. 1993. Analytical model for extracting intrinsic fluorescence in a turbid media. *Appl. Opt.* 32:3585–3595.